



THREE-DIMENSIONAL VELOCITY STRUCTURE OF THE CRUST IN CENTRAL LAKE BAIKAL FROM LOCAL SEISMIC TOMOGRAPHY

L.Yu. Eponeshnikova ^{1,2✉}, A.A. Duchkov ^{1,2}, D.P.-D. Sanzhieva ^{3,4}, S.V. Yaskevich ⁵

¹Trofimuk Institute of Petroleum Geology and Geophysics, Siberian Branch of the Russian Academy of Sciences, 3 Academician Koptug Ave, Novosibirsk 630090, Russia

²Novosibirsk State University, 1 Pirogov St, Novosibirsk 630090, Russia

³Dobretsov Geological Institute, Siberian Branch of the Russian Academy of Sciences, 6a Sakhyanova St, Ulan-Ude 670047, Republic of Buryatia, Russia

⁴Buryat Branch of the Federal Research Center of the Geophysical Survey, Russian Academy of Sciences, 6a Sakhyanova St, Ulan-Ude 670047, Republic of Buryatia, Russia

⁵Institute of the Earth's Crust, Siberian Branch of the Russian Academy of Sciences, 128 Lermontov St, Irkutsk 664033, Russia

ABSTRACT. This work deals with the importance of studying seismicity and deep structure of the Earth's crust in the region of the Baikal rift zone. The study presents a three-dimensional velocity structure of the Earth's crust in the central part of Lake Baikal, obtained from the results of tomographic inversion of the travel times of P- and S-waves from more than 800 seismic events. Synthetic tests provide substantiation for the resolution of the tomographic inversion algorithm. The seismic structure of the crust was obtained to a depth of 35 km and has a direct relationship with the geological structure. The three-dimensional distributions of seismic P- and S-wave velocity anomalies are in good agreement with each other.

The sharp contrast between the anomalies may indicate a difference in the material composition of the basement of the Central Baikal basin. At a 15-km depth below the Selenga River delta, there is observed a strong low-velocity anomaly which confirms the presence of a thick sedimentary cover therein. In the basement (at depths of 20 km or greater), to the northeast of the intersection between the Delta fault and the Fofanov fault, there occurs a high-velocity anomaly elongated towards the Olkhon Island. This anomaly is probably related to a rigid block in the earth's crust. The same depths, on the western side of the Baikal-Buguldeika fault, show a reduced V_p/V_s ratio: 1.56–1.65 versus 1.70–1.75 in the adjacent areas. This indicates another type of basement rock composition and the presence of consolidated matter there.

Besides, there has been made a more accurate hypocenter determination for further comparison between seismic events and active fault structures. For the central part of Lake Baikal, the distribution of seismicity mainly corresponds to depths of 10–22 km. The situation is different below the Selenga Delta – the only area where seismicity is observed at depths greater than 22 km, – which can be attributed to complex fault interactions.

The velocity anomalies discussed herein are confined to reliably identified active faults and correlate well with the distribution of seismicity and gas hydrate structures.

KEYWORDS: Baikal rift zone; Central Baikal basin; local seismicity; seismic tomography; Earth's crust

FUNDING: The work was done as part of research project AAAA-A19-119102490050-2 IGG SB RAS and state assignment 075-01471-22, with the use of the data obtained from the Large-Scale Research Facilities "Seismic and infra-sound monitoring of the Arctic cryolite zone and continuous monitoring of the Russian Federation, adjacent areas and the world".



RESEARCH ARTICLE

Correspondence: Lyubov Yu. Eponeshnikova, eponeshnikovalu@ipgg.sbras.ru

Received: March 4, 2022

Revised: May 4, 2022

Accepted: May 16, 2022

FOR CITATION: Eponeshnikova L.Yu., Duchkov A.A., Sanzhieva D.P.-D., Yaskevich S.V., 2023. Three-Dimensional Velocity Structure of the Crust in Central Lake Baikal from Local Seismic Tomography. *Geodynamics & Tectonophysics* 14 (1), 0683. doi:10.5800/GT-2023-14-1-0683

1. INTRODUCTION

The Baikal Rift Zone (BRZ) is one of the largest continental divergent boundaries. It is characterized by active rifting and the occurrence of lithospheric extension processes. The BRZ includes large lithospheric blocks: Siberian Platform, Amur Plate, and East Sayan, Mongolian and other microplates [Logachev, 2001]. The Global Positioning System (GPS) data show that the Baikal rift is opening at a rate of 3–4 mm yr [Ashurkov et al., 2011, 2016; Calais et al., 2003; Lukhnev et al., 2013; Sankov et al., 2003]. The collision between the Indian Plate and the Eurasian Plate is evident in the fact that the lithosphere moves in the northeastern and latitudinal directions relative to the Siberian Platform. The Siberian Platform moves very slowly north, and the Amur Plate moves more rapidly southeast [Ashurkov et al., 2011].

No consensus exists on the causes of rifting, although there is no doubt that the BRZ is a tectonically active area. Active tectonic processes reflect the existence of a complex fault system and seismicity [Logachev, 1999, 2003; Sherman, Levi, 1977; Levi et al., 1995, 1997; Sherman et al., 2012]. Continental rifting is usually accompanied by volcanic and magmatic activities. However, the BRZ volcanism evidence was only found for the Neogene period, and there was a decrease in volcanic activity in the Quaternary [Logachev, Zorin, 1987].

The study area is confined to the Central Baikal basin (Fig. 1). There lies a delta of the Selenga River which is the largest continental delta and a depocenter of Lake Baikal, with about an 8 km thick sediment layer [Hutchinson et al., 1992; Scholz, Hutchinson, 2000]. The Selenga River delta is a depression with a complex fault-block structure and high seismic activity. According to the data on focal mechanisms of large earthquakes, the key role therein is played by the lithospheric extension processes [Misharina, Solonenko, 1972, 1977; Misharina et al., 1983; Melnikova, Radziminovich, 1998]. A complex geodynamic environment in the Selenga River delta is due to the mutually intersecting Delta, Fofanov and Sakhalin-Enkhaluk faults [Lunina et al., 2009].

This paper considers local earthquake tomography which allows a velocity model and earthquake hypocenters to be simultaneously refined based on the P- and S-wave arrival times [Nolet, 1990]. For the Baikal region, there were created several tomographic models [Kulakov, 1999, 2008; Mordvinova et al., 2000; Burkholder et al., 1995; Gao et al., 2003; Petit et al., 1998; Tiberi et al., 2003; Yakovlev et al., 2007; Zhao et al., 2006] which have similar characteristics (high velocities for the Siberian Platform and low-velocity anomalies for the upper mantle of the South Baikal basin) but may differ in detail. Based on the results of the studies conducted using local data [Kulakov, 1999; Petit et al., 1998], beneath the Baikal folded area, up to a depth of 20 km, there can be found a large negative anomaly that changes to positive one. In [Yakovlev et al., 2007], the regional data were used to obtain the crustal and upper-mantle velocity anomalies. According to the results obtained, the authors identify negative anomalies

coinciding with the Cenozoic volcanic areas. The above-mentioned results, however, do not provide information on the detailed structure of the Earth's crust in the area we are interested in.

This paper discusses three-dimensional velocity-structure determination of the crust in the Central Baikal basin by local seismic tomography with simultaneous refinement of hypocenter parameters of the earthquakes. Local seismic tomography reveals block structure of the earth's crust, thus providing insight into the understanding of tectonic processes in the study area. The results obtained herein make it possible to consider in more detail the crustal velocity structure of the Central Baikal, as compared to previous seismic tomography studies conducted in the Baikal region.

2. GEOLOGICAL AND GEOPHYSICAL DESCRIPTION OF THE STUDY AREA

There are two major hypotheses about the formation of the BRZ. These are the concepts of active and passive rifting.

The idea of active rifting is related to the presence of mantle plume beneath the Baikal which causes lithospheric uplift and extension [Logachev, 1993; Logachev, Zorin, 1987; Zorin, Turutanov, 2005]. One indication that this theory might be right is the existence of high heat flow – the heat flow in the BRZ is variable (from 40 to 200 mWt/m²) but tends to be greater than the mean value [Golubev, 2007; Duchkov, Sokolova, 2014]. Based on the deep seismic sounding (DSS) data, evidence was also found for the asthenosphere low-velocity protrusion (7.7–7.8 km/s) beneath the Baikal which is interpreted as an anomalous mantle [Song et al., 1996]. In accordance with the gravimetric data, positive anomalies of the Bouguer reduction are the indicator of basic-ultrabasic igneous rock intrusions [Khain, Lomize, 2005; Gao et al., 1997], negative anomalies correspond to large-scale mantle inhomogeneities [Dobretsov et al., 2019].

Another factor to be considered is passive rifting. This model is based on plate interactions which cause the lithosphere extension. According to this concept, the extension is due to the collision between the Indian plate and the Eurasian plate, and to the subduction of the Pacific plate [Nicolas et al., 1994; Peltzer, Tapponnier, 1988; Zonenshain, Savostin, 1981]. There are also combined theories of the rift formation which imply two to three formation stages [Logachev, 2003; Achauer, Masson, 2002; Chemenda et al., 2002; Lesne et al., 2000; Mats, 2012, 2015; Petit et al., 1998].

The Baikal basin is the largest part of the BRZ. There can be distinguished three main basins of Lake Baikal – South, Central and North [Logachev, 2003]. The estimates of sediment thickness reported for the Baikal basin are different. The seismic reflection survey (SRS) of the lake yielded sediment layer thicknesses ranging from 7 to 8 km in the North and Central basins [Hutchinson et al., 1992]. Seismic refraction profiles (SRP) obtained in the Central basin showed that the sediments therein are up to 9.5 km

thick [Ten Brink, Taylor, 2002]; the greatest depth to basement – up to 14 km – was obtained for the South basin [Suvorov, Mishen'kina, 2005].

The coast of Lake Baikal is composed of heterochronous rocks. The western shoreline of the Baikal is composed primarily of the Archean and Archean-Proterozoic basement and sedimentary complexes of the Siberian Platform,

and the eastern – by the Phanerozoic rocks of the Sayan-Baikal Fold Belt [State Geological Map..., 2009; Gvozdkov, 1998; Grudin, Chuvashova, 2011]. Among the synrift sediments of the Baikal region are the Upper Cretaceous Cenozoic rocks whose accumulation period corresponds to rifting and Lake Baikal basin formation times [Mats, 2012]. The Upper Cretaceous–Paleogene deposits which

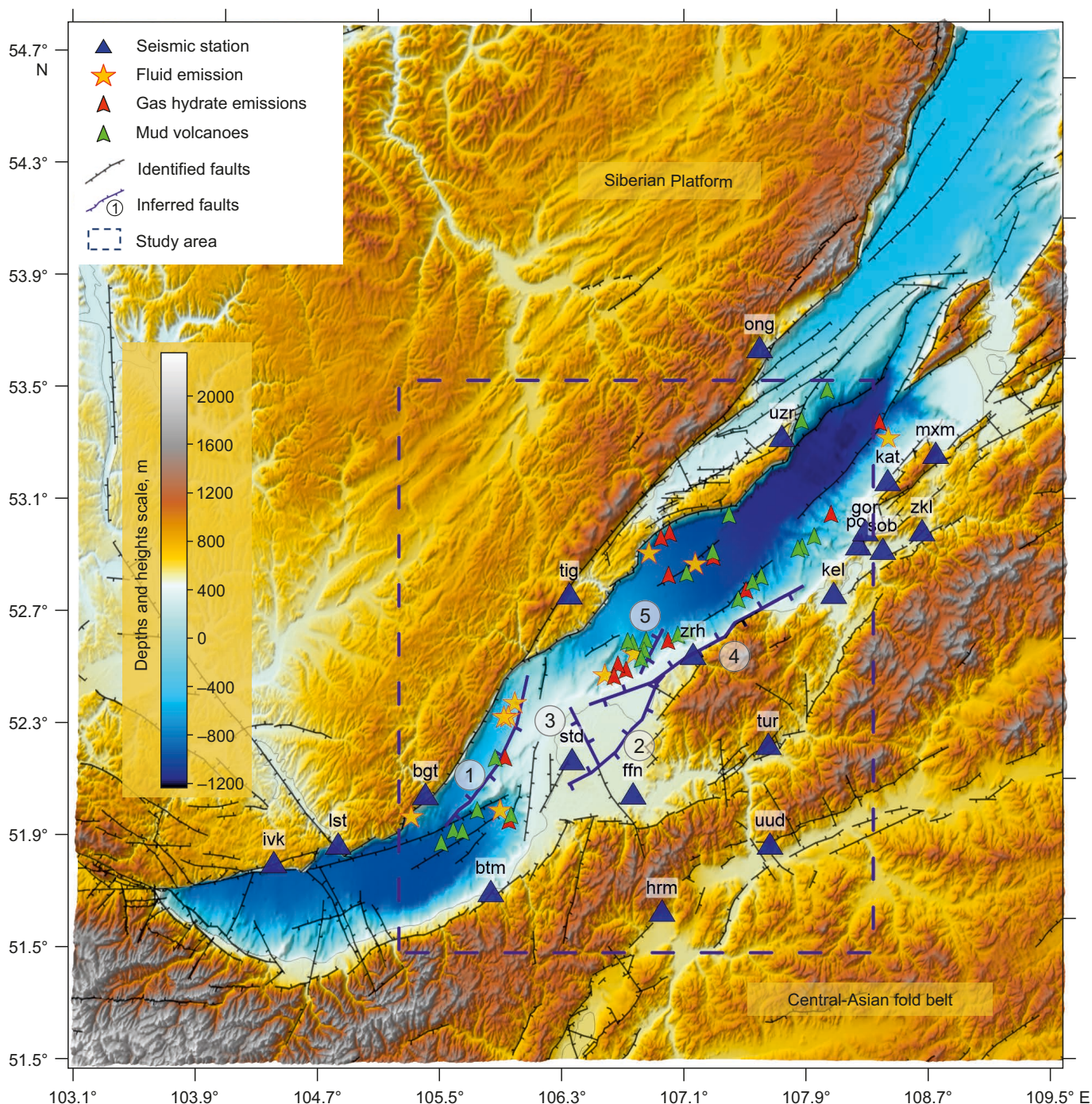


Fig. 1. Map of relief and main structural and tectonic elements in the area of the Baikal depression.

The map shows reliably identified Pliocene-Quaternary faults [Lunina, 2016]. Numbers in circles correspond to the faults under discussion: 1 – Baikol-Buguldeika, 2 – Delta, 3 – Fofanov, 4 – Sakhalin-Enkhaluk, 5 – unnamed.

Green and red marks represent mud volcanoes and gas hydrate emissions, respectively. Fluid ejections are shown by yellow stars [Khlystov et al., 2018]. Seismic stations correspond to blue triangles. The herein-considered area is shown as blue dashed lines. Digital elevation model for Lake Baikal was taken from <https://www.gebco.net/> where the data is freely available.

are lacustrine or alluvial in origin occur within the Selenga River delta and Olkhon Island [Logachev, 1974; Mats, 2012, 2015]. The Quaternary deposits which are widespread in all intermountain and submontane troughs have been derived from different types of soft rocks and are of different geneses. A detailed outline of the Cenozoic deposits within the Baikal basin is provided in [Mats et al., 2001]. In view of the diversity of rocks bordering the lake, it could be assumed that the Baikal basement has a complex uneven-aged block structure.

The study area is confined to the Central Baikal basin. The important structures therein are the Delta, Fofanov and Sakhalin-Enkhaluk faults.

The Delta fault in the estuary part of the Selenga River (Fig. 1) is the major seismoactive structure there [Lunina et al., 2012], with normal-fault kinematics. The displacement along the fault occurred under the NW-SE extension conditions. The activation of this fault is due to the Tsagan earthquake of 1862, which gave rise to the formation of the Proval Bay. The formation and evolution of the Proval Bay have been described in detail in [Shchetnikov et al., 2012], in the context of the analysis of common morphological characteristics of the Baikal rift.

Orthogonally to the Delta fault, there runs the Fofanov fault (Fig. 1). This fault penetrates deeply into the crust up to the upper mantle [Solonenko, 1981] and is identified through the geomagnetic survey. The fault separates the blocks with different depths to basement; according to [Lunina et al., 2009, 2010], it is the right-lateral strike-slip fault with its highly seismic northern part.

The Sakhalin-Enkhaluk fault (Fig. 1) intersects with the Delta fault on the coast near the northeastern Proval Bay, strikes northeast, and is interpreted as a normal fault. It belongs to the most seismically active faults; with numerous thermal springs thereon [Solonenko, 1981; Lunina et al., 2009].

Geodynamic complexity of the Selenga River delta is determined by the mutually intersecting Delta, Fofanov and Sakhalin-Enkhaluk faults [Lunina et al., 2009]. It is worthy of note that the seismicity of these faults occurs at depths greater than 22 km, whereas in the rest of the Central Baikal basin it is confined to depths of 10–22 km [Radziminovich, 2010; Suvorov, Tubanov, 2008]. According to the electromagnetic monitoring data, the Selenga River delta has a mosaic (block) structure with alternating uplifted and subsided small blocks [Nevetrova, Epov, 2004; Lunina et al., 2009].

The objects of interest in the avandelta of the Selenga River are the Posolsk Bank and Kukui Ridge. They are tectonically uplifted blocks which previously were the parts of the surface in the Selenga River delta and are adjacent to the same fault [Logachev, 2003]. In [Khlystov et al., 2016], it is reported about an abrupt activation of seismotectonic activity about 1.0–0.8 million years ago which resulted in the separation of the Posolsk Bank and Kukui Ridge from the Selenga River delta and in their further autonomous existence. On the southeast of the ridge, there is a canyon whose formation can be attributed to rifting

processes which is evidenced by sharp river bends and step-like canyon slopes. The Kukui Canyon is also known for a large concentration of mud volcanoes and gas hydrates [Khlystov et al., 2018].

The Central Baikal basin is characterized by high seismicity. The most seismically active area is the Selenga River delta. Seismicity distribution in the Baikal area has been considered in many studies since the 1960s (in the works of Treskov, Misharina Golenetsky, Vertlib, Krylov and other scientists). The studies provide evidence that the major earthquakes are confined to depth interval 0–10 km [Krylov, 1980] or 5–20 km [Golenetsky, Perevalova, 1988]; in some of the studies, the source depths are estimated at 30 [Déverchère et al., 1991] or even at 40 km [Déverchère et al., 2001; Gileva et al., 2000]. In [Suvorov, Tubanov, 2008], there was obtained the distribution of seismic sources beneath the Central Baikal in the context of the velocity model based on the DSS data which made it possible to identify a seismically active layer going down under the Selenga depression. A similar result was provided in [Radziminovich, 2010].

3. SEISMIC TOMOGRAPHY DATA AND METHOD

This paper deals with travel times for straight waves (Pg and Sg) recorded at 20 seismic stations. These stations belong to the Baikal and Buryat branches of the FRC UGS RAS. The seismological network is extended along the Baikal and characterized by an irregular distribution of seismic stations. The processing has been performed on the data catalogue containing the travel times of P- and S-waves from local earthquakes over the period 2001–2011. The energy class K for this data sample ranges from 6.5 to 12.2. Fig. 2 shows a seismological network configuration and seismicity distribution. The processing involved seismic records obtained from at least 5 stations located on a maximum distance of 100 km away from the epicenter. After the catalog processing, there were 826 events left, with the travel times of Pg-waves (6406) и Sg-waves (6461).

The paper deals with LOTOS – Local Tomography Software [Koulakov, 2009]. It allows a 3D velocity model and earthquake hypocenters to be simultaneously refined based on P- and S-wave travel times. Travel time calculations and tomographic inversion were based on ray tracing. The tomographic inversion is performed in several iterations, each of which includes more accurate hypocenter determination, and tomographic matrix calculation and inversion. More details on more concrete implementation of the algorithms are provided in [Kulakov, 1999; Koulakov et al., 2002]. The iterative process continues as long as dispersion misfit is constant (decreases by less than 3–5 %). In the present work, the inversion process converged usually after three iterations.

Fig. 3 shows the distribution of rays in the study area and the nodal parametrization of velocity model. An area with sufficient ray coverage implies the in-principle possibility of reconstructing velocity model. It is evident that the coverage area includes the Central basin, northern

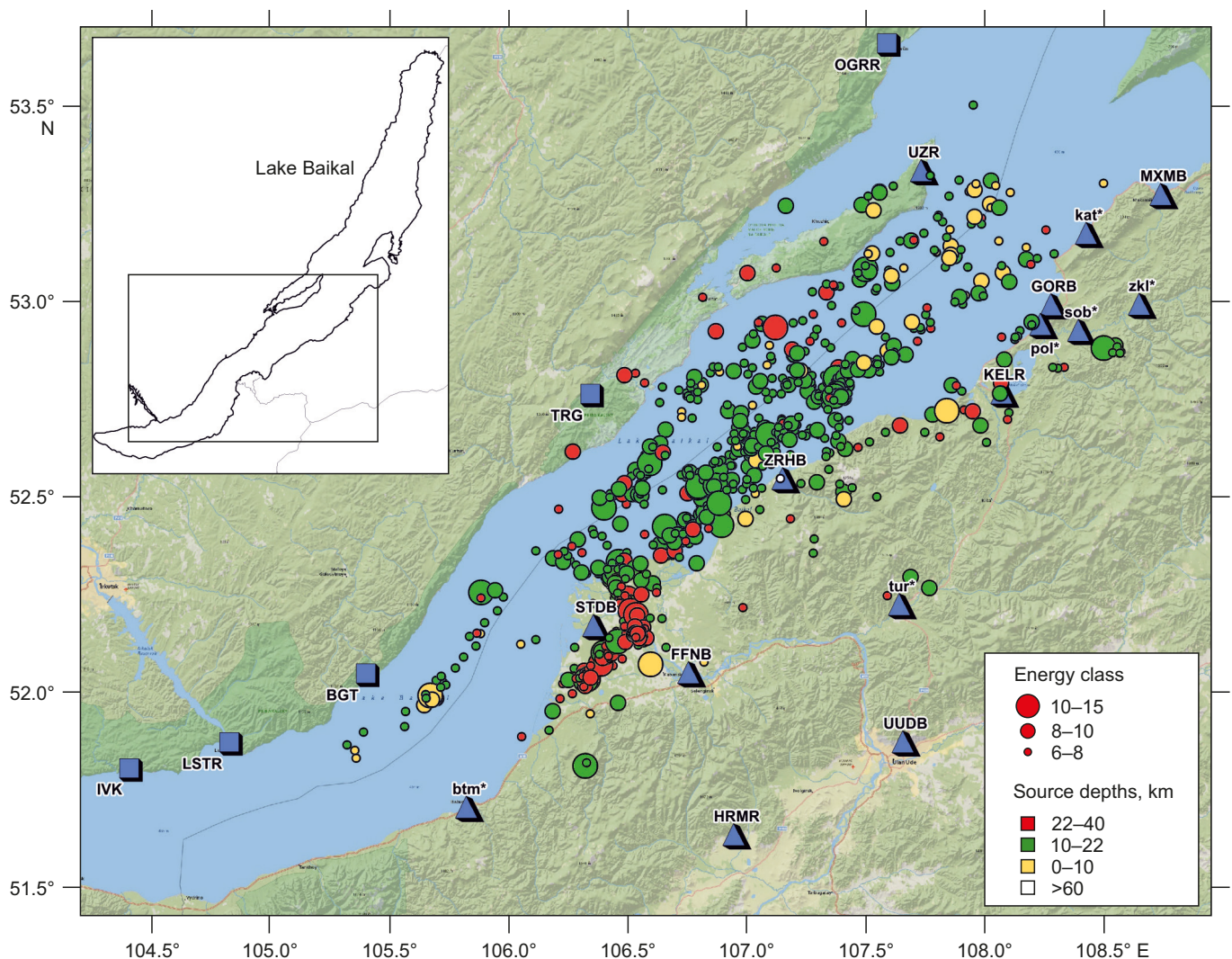


Fig. 2. Distribution of seismicity in the study area (the epicenters are shown after their more precise determination during tomographic inversion).

Triangles are seismic stations of the Buryat Branch of the FRC UGS RAS (* – the regional (local) code of the station), squares are the stations of the Baikal Branch of the FRC UGS RAS. In the insert, the rectangle shows the studied area.

South basin, and a part of the southeastern coast. It has to be noted that the LOTOS algorithm puts emphasis on reducing the influence of the distribution of nodes of parametrization grid on the results. To do this, there has been performed an inversion using different grid orientations (0°, 22°, 45° and 67° in our case). After the results for different grid orientations are calculated, they are summarized in a single model reducing any artifacts related to grid orientation.

The result of tomographic inversion depends on the choice of regularization parameters of smoothing and amplitude damping. Optimal parameters are selected based on synthetic tests. Large parameter values ensure uniqueness and sustainability of the solution but smooth it, thus reducing the level of detail of the model obtained. Small parameter values are the causes of unsustainability of the solution – in the model there appear velocity anomalies which have little impact on travel times as they are not driven by data. In App. 1 there are presented the results

of checkboard tests. First, these tests allow determining optimal regularization parameters (absence of any other anomalies in the models obtained). Second, they allow determining resolution of the observation system involved, i.e. the area and the dimensions of velocity anomalies which are reliably reconstructed for the available seismicity distribution and station location. Based on the test results, it was concluded that interpretable anomalies are those which have horizontal dimensions 30 km or greater (App. 1, Fig. 1.1).

For ray tomography it is important to choose the initial velocity model because its proximity to the true model provides precise tomography inversion results. It was based on the one-dimensional model of the Earth's crust derived from the DSS method [Song et al., 1996]. Then the model was refined using LOTOS software tools (the one-dimensional model was refined so that the velocity anomalies had a mean of zero at all depths. As a result, there was obtained the initial velocity model shown in

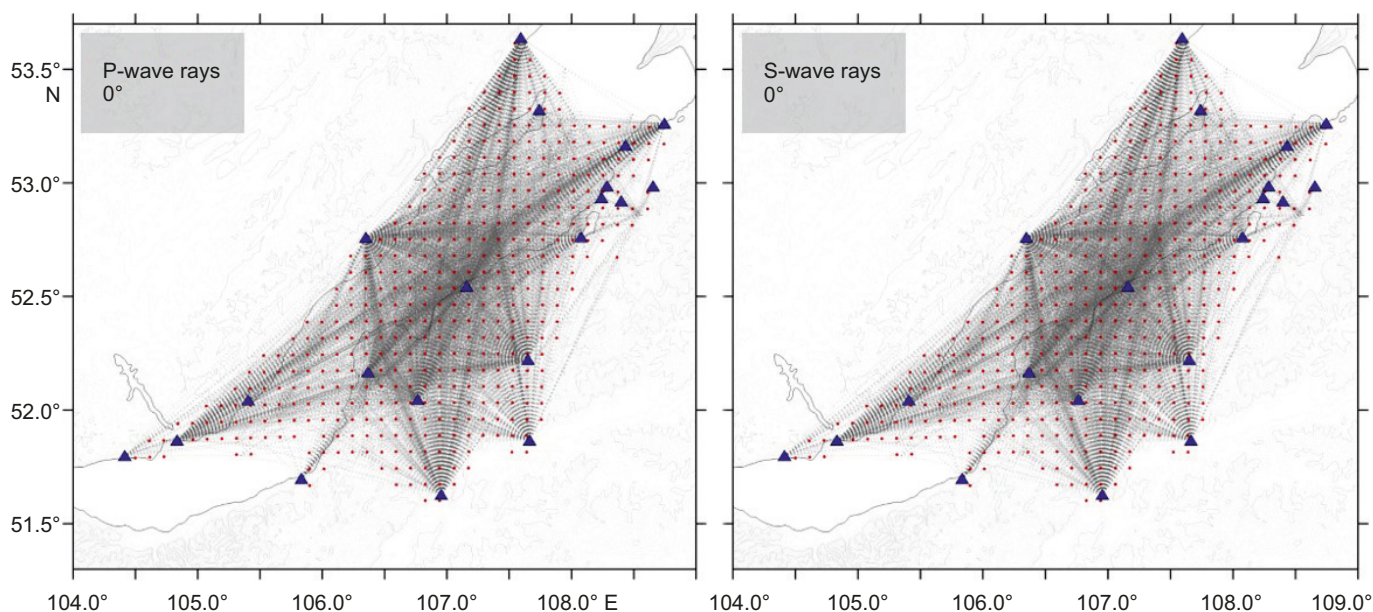


Fig. 3. Distribution of P- and S-wave rays (gray lines), seismic stations (blue triangles) and nodes of parameterization grids with orientation of 0° (red dots).

Table 1 (the velocity between the presented depths is linearly approximated).

4. TOMOGRAPHIC INVERSION RESULTS

At first there were obtained the preliminary results of earthquake hypocenters from the one-dimensional model, and then there were performed three iterations of tomographic inversion. Root-mean-square misfits of P- and S-wave travel times after each of the iterations are presented in [Table 2](#). After the third iteration, the misfits reduced to 0.22 s (for P-waves) and 0.30 s (for S-waves).

Tomographic inversion produced the three-dimensional distribution of P- and S-wave velocity anomalies shown on horizontal ([Fig. 4](#)) and vertical ([Figs 5, 6](#)) sections. The figures show that most of the P- and S-wave velocity anomalies correspond well to each other. The dots in [Fig. 4, 5](#) and [6](#) stand for the refined locations of sources (after inversion); the vertical sections (see [Fig. 5; Fig. 6](#)) show the sources in a 7-km wide layer around corresponding sections (refined epicenters for the whole catalogue are shown in [Fig. 2](#)). [Table 3](#) presents the distribution of sources along the depth. It can be seen that most of the earthquakes occur at depths of 10–22 km and coincide with the estimates reported in [[Radziminovich, 2010; Suvorov, Tubanov, 2008](#)]. The Selenga River delta exhibits the concentration of earthquakes with hypocenter depths to 30 km. An earthquake near Zarechye (ZRHB) station occurred at a depth of >60 km (see [Fig. 2](#)).

5. RESULTS AND DISCUSSION

[Fig. 7](#) presents a comparison between the results obtained for velocity anomalies and reliably identified faults [[Lunina, 2016](#)].

Anomalous area 1 shown in [Fig. 7](#) is located northwest of the Selenga River delta. According to the seismic data

[[Hutchinson et al., 1992](#)], there lies the subsided block of the acoustic basement with a sediment thickness of about 7.5 km. On the southeast, this area is bounded by the Baikal-Buguldeika fault – a normal-fault [[Lunina, 2016](#)] which is considered active since it is confined to both seismicity and gas hydrate structures [[Khlystov et al., 2016, 2018](#)]. The fault separates area 1 from the adjacent low-rate block (from S-velocity anomalies) which is characterized by low seismicity (in accordance with the regional catalog data over the period 1960–2021); there is also located the Posolsk Bank. A new result is that the area shows an anomalously low V_p/V_s ratio (1.56–1.65) as compared to the surrounding rock (1.70–1.75) ([Fig. 7, c](#)). Therefore, it can be concluded that the blocks on either side of the Baikal-Buguldeika fault not only move relative to each other but also differ in their physical composition.

Area 2 is located northeast of the intersection between the Delta and Fofanov faults and elongated towards the Olkhon Island ([Fig. 7](#)). According to the seismic tomography data, there lies a high-velocity rigid crustal block at a depth of about 20 km which is presumably composed of the rocks different from the host rock in composition.

This anomalous block and seismicity distribution there-around can be seen clearly in the vertical section along Profile 5 (see [Figs 5, 6](#)). The block is ~80–100 km long and ~20 km wide and lies at depths of 15 to 35 km. Seismicity is mostly concentrated on the boundary between the low- and high-wave-velocity areas at depths of 15 to 20 km.

Seismicity (hypocenter) distribution analysis shows that there occurs a complex interaction between this block and adjacent structures ([Fig. 7](#)). Seismicity is concentrated along the southeastern margin of the rigid block. There is a clearly defined arc structure similar to the Baikal-Buguldeika fault mentioned above. It has a submeridional strike and is formed by the southern Delta fault and Fault 5 in [Fig. 7](#)

Table 1. Initial Velocity Model

Depth, km	Vp, km/s	Vs, km/s
-2	5.14	2.99
5	5.67	3.40
10	6.03	3.54
15	6.20	3.60
20	6.34	3.67
30	6.49	3.82
40	7.13	4.15

Table 2. Average misfits of arrival times (s)

Iteration No	dtP, s	dtS, s
1	0.29	0.49
2	0.22	0.31
3	0.22	0.30

Table 3. Depth distribution of seismicity after tomographic inversion

Depth, km	Number of events
0-10	65
10-22	593
22-40	167
>60	1

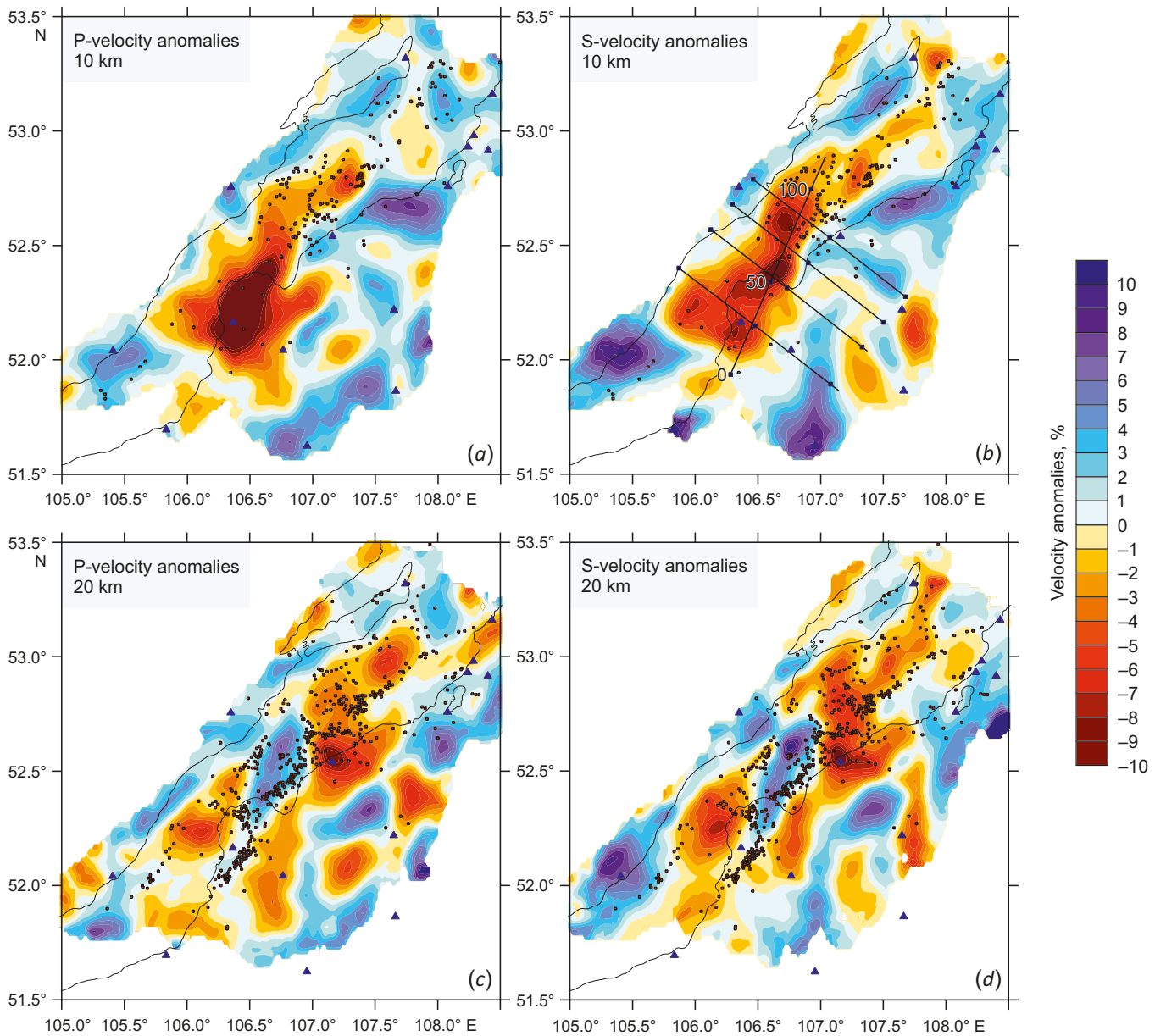


Fig. 4. P- and S-velocity anomalies from tomographic inversion. Horizontal sections at depths of 10 km (a, b) and 20 km (c, d); dots denote the events at corresponding depths; triangles denote seismic-station locations. The location of the profiles for constructing vertical sections is indicated in the fragment (b).

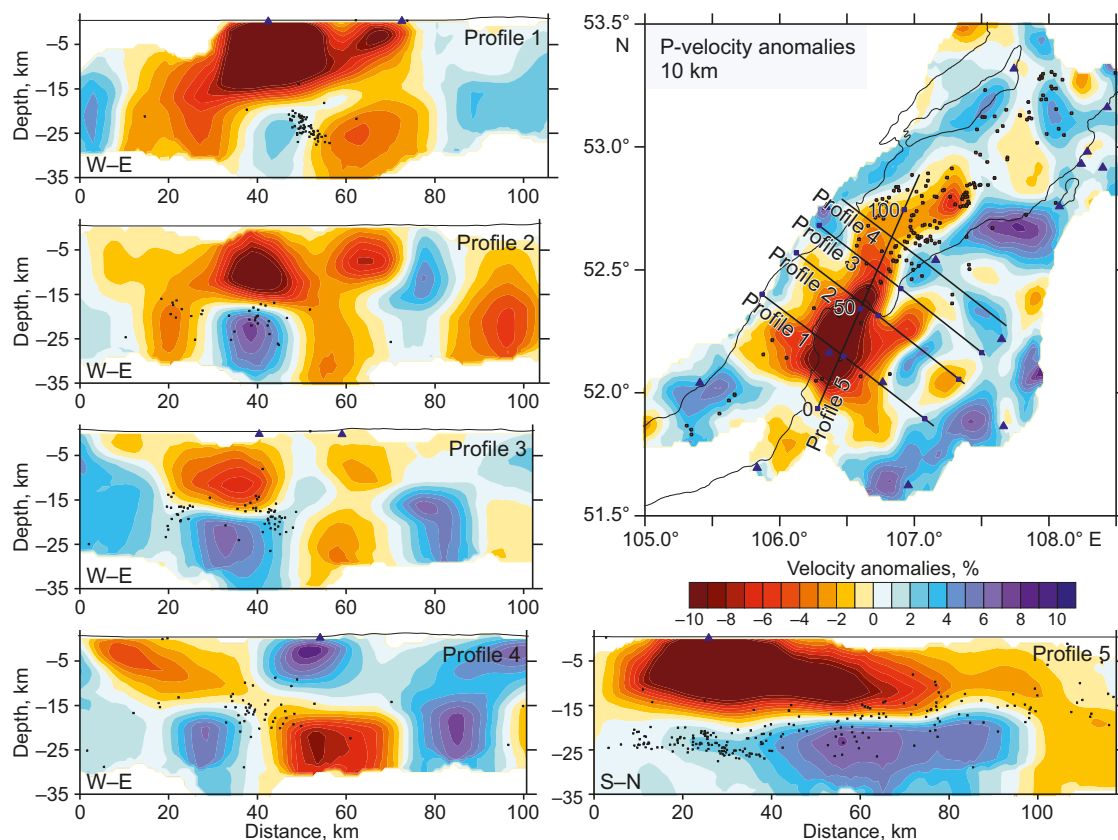


Fig. 5. P-velocity anomalies from tomographic inversion (vertical sections). Dots denote the events near the section (within a 7-km layer); triangles denote seismic-station locations. Vertical section lines are shown in the upper right panel.

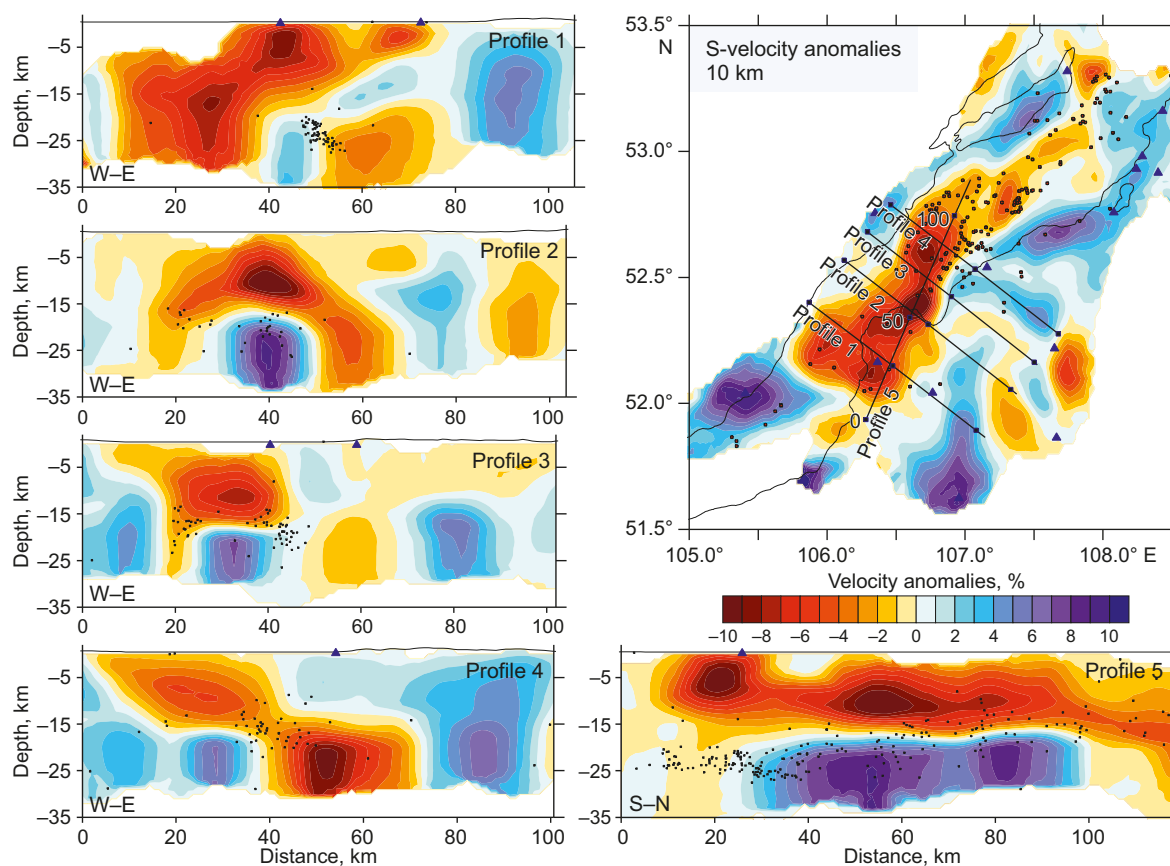


Fig. 6. S-velocity anomalies from tomographic inversion (vertical sections).

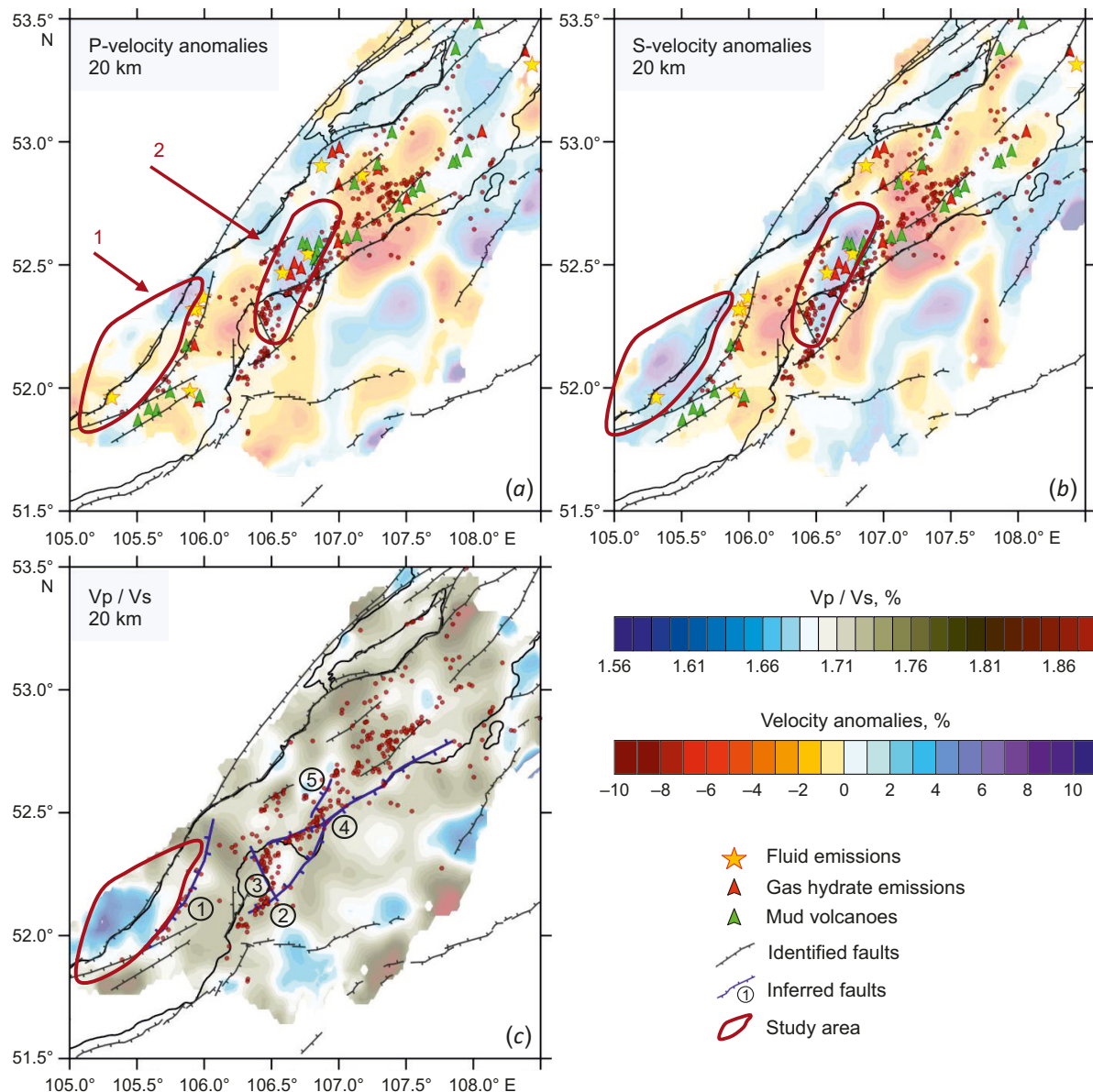


Fig. 7. Interpretation of the results of tomographic inversion.

Vp (a) and Vs (b) anomalies and the Vp/Vs ratio (c) at a depth of 20 km; the dots stand for seismicity around 20-km depth. The lines show the reliably identified Pliocene-Quaternary faults [Lunina, 2016]. Numbers in circles correspond to the faults: 1 – Baikal-Buguldeika, 2 – Delta, 3 – Fofanov, 4 – Sakhalin-Enkhaluk, 5 – unnamed. The discussed regions are shown by red contours.

which continues into the Baikal water area and is traced by exposed gas hydrates and underwater volcanic eruptions [Khlystov et al., 2018]. There also lies the Kukui Canyon – the longest canyon on the Baikal bottom – whose complex tortuous shape can be partially attributed to the fault pattern [Khlystov et al., 2016].

Not all southeastern margin of the high-velocity block is seismically active. Seismicity is only observed for the southern Delta fault. This appears to be related to the Sakhalin-Enkhaluk fault cutting thorough the high-velocity block in the southwestern direction. The block seems to be fractured along this line since the seismicity is now occurring throughout the block rather than on the block margin. According to [Solonenko, 1981; Lunina et al., 2009], there are many thermal springs along this fault. Besides,

seismicity is observed on the southwestern margin of the Fofanov fault.

Therefore, this implies a complex interaction between the crustal blocks therein which may have resulted from the overlapping stages in the development of the Baikal rift [Mats, 2012]. The feature of the interaction considered is emphasized by large depths of the hypocenters confined to the Delta and Fofanov faults (22–30 km), but there is almost no earthquake activity at these depths in the rest of the study area.

The revealed contrast between P- and S-velocity anomalies (sections for 20 km depth in Fig. 4) generally indicate a significant difference in composition of basement rocks in the Baikal basin. The geological studies show that the Baikal borders are composed of heterochronous rocks. For

example, on the western coast near area 1 there are outcrops of the Archean-Proterozoic migmatites and crystalline schists alternating with the Neoproterozoic sediments. The eastern coast of the Baikal is mostly composed of the Phanerozoic rocks [State Geological Map..., 2009; Gvozdkov, 1998; Grudin, Chuvashova, 2011]. In the Selenga River delta and the Olkhon Island, there occur Upper Cretaceous–Paleogene lacustrine and alluvial deposits [Logachev, 1974; Mats, 2012, 2015]. Therefore, a wide variety of lake-bordering rocks suggests that the Baikal basement has a complex heterochronous block structure. This allows interpreting the revealed contrasts between seismic-wave velocity anomalies and their relationship as heterochronous blocks.

6. CONCLUSION

Seismic tomography method presented herein yielded the three-dimensional distribution of P- and S-velocity anomalies and provided better location estimates for hypocenters in the Central Baikal basin. The study was conducted based on the catalog of regional seismic events recorded in 2001–2012. A data set provides sufficient ray coverage of the study area and reliable identification of anomalies with horizontal dimensions from 30 km.

Northeast of the intersection between the Delta fault and the Fofanov fault, there is a high-velocity anomaly elongated towards the Olkhon Island. This anomalous area is interpreted as a rigid crustal block. This block is 80–100 km long and about 20 km wide, with a depth of occurrence from 15 to 35 km. This block is cutting through the Sakhalin-Enkhaluk fault, which provides a complex interaction between the crustal blocks therein. The feature of interaction is emphasized by large depths of the hypocenters confined to the Delta fault and the Fofanov fault, but there are almost no earthquakes that occur at these depths in the rest of the area.

In the southwest of the study area, there is a range of high S-wave velocities. Anomalously low V_p/V_s ratios imply that this anomaly is a basement block which differs from the surrounding rock in material composition. This block underwent subsidence, as can be inferred from a 7.5-km increase in the thickness of bottom sediments thereabove. In the southeast, the block is bounded by the Baikal-Buguldeika fault which presumably separates heterochronous basement blocks.

Thus, there were obtained new data on the block structure of the Earth's crust beneath the Baikal basin that might be used for constructing geological and tectonic models of the Baikal rift.

7. ACKNOWLEDGEMENT

The authors express their gratitude to Ts.A. Tubanov for the data provision, recommendations on improving research, and constructive comments.

8. CONTRIBUTION OF THE AUTHORS

Data processing, results interpretation, manuscript and graphic preparation – Eponeshnikova L.Yu.; results

interpretation, manuscript revision – Duchkov A.A.; manuscript and graphic revision – Sanzhieva D.P.-D., Yaskevich S.V. All authors read and approved the final manuscript.

9. DISCLOSURE

The authors declare that they have no conflicts of interest relevant to this manuscript.

10. REFERENCES

- Achauer U., Masson F., 2002. Seismic Tomography of Continental Rifts Revisited: From Relative to Absolute Heterogeneities. *Tectonophysics* 358 (1–4), 17–37. [https://doi.org/10.1016/S0040-1951\(02\)00415-8](https://doi.org/10.1016/S0040-1951(02)00415-8).
- Ashurkov S.V., Sankov V.A., Miroshnichenko A.I., Lukhnev A.V., Sorokin A.P., Serov M.A., Byzov L.M., 2011. GPS Geodetic Constraints on the Kinematics of the Amurian Plate. *Russian Geology and Geophysics* 52 (2), 239–249. <https://doi.org/10.1016/j.rgg.2010.12.017>.
- Ashurkov S.V., Sankov V.A., Serov M.A., Luk'yanov P.Y., Grib N.N., Bordonskii G.S., Dembelov M.G., 2016. Evaluation of Present-Day Deformations in the Amurian Plate and Its Surroundings, Based on GPS Data. *Russian Geology and Geophysics* 57 (11), 1626–1634. <https://doi.org/10.1016/j.rgg.2016.10.008>.
- Burkholder P.D., Meyer R.P., Delitsin L.L., Davis P.M., Zorin Yu.A., 1995. A Teleseismic Tomography Image of the Upper Mantle beneath the Southern Baikal Rift Zone. In: *Proceeding of the XXI General Assembly of the International Union of Geodesy and Geophysics* (July 2–14, 1995, Boulder, Colorado, USA). IUGG, 400 p.
- Calais E., Vergnolle M., Sankov V., Lukhnev A., Miroshnichenko A., Amarjargal S., Déverchère J., 2003. GPS Measurements of Crustal Deformation in the Baikal-Mongolia Area (1994–2002): Implications on Current Kinematics of Asia. *Journal of Geophysical Research: Solid Earth* 108 (B10), 2501. <https://doi.org/10.1029/2002JB002373>.
- Chemenda A., Déverchère J., Calais E., 2002. Three-Dimensional Laboratory Modelling of Rifting: Application to the Baikal Rift, Russia. *Tectonophysics* 356 (4), 253–273. [https://doi.org/10.1016/S0040-1951\(02\)00389-X](https://doi.org/10.1016/S0040-1951(02)00389-X).
- Déverchère J., Houdry F., Diamant M., Solonenko N.V., Solonenko A.V., 1991. Evidence for a Seismogenic Upper Mantle and Lower Crust in the Baikal Rift. *Geophysical Research Letters* 18 (6), 1099–1102. <https://doi.org/10.1029/91GL00851>.
- Déverchère J., Petit C., Gileva N., Radziminovitch N., Melnikova V., Sankov V., 2001. Depth Distribution of Earthquakes in the Baikal Rift System and Its Implications for the Rheology of the Lithosphere. *Geophysical Journal International* 146 (3), 714–730. <https://doi.org/10.1046/j.0956-540x.2001.1484.484.x>.
- Dobretsov N.L., Buslov M.M., Vasilevsky A.N., 2019. Geodynamic Complexes and Structures of Transbaikalia: Record in Gravity Data. *Russian Geology and Geophysics* 60 (3), 254–266. <https://doi.org/10.15372/RGG2019021>.
- Duchkov A.D., Sokolova L.S., 2014. Heat Flow in Siberia. In: *Geophysical Methods for the Study of the Earth's Crust. Proceedings of the All-Russian Conference Dedicated to the*

100th Anniversary of the Birth of Academician N.N. Puzyrev. Institute of Petroleum Geology and Geophysics, Novosibirsk, p. 211–216 (in Russian) [Дучков А.Д., Соколова Л.С. Тепловой поток Сибири // Геофизические методы исследования земной коры: Материалы Всероссийской конференции, посвященной 100-летию со дня рождения академика Н.Н. Пузырева (8–13 декабря 2014 г.). Новосибирск: ИИГГ СО РАН, 2014. С. 211–216].

Gao S., Davis P.M., Liu H., Slack P.D., Rigor A.W., Zorin Y.A., Logatchev N.A., 1997. SKS Splitting beneath Continental Rift Zones. *Journal of Geophysical Research: Solid Earth* 102 (B10), 22781–22797. <https://doi.org/10.1029/97JB01858>.

Gao S.S., Liu K.H., Davis P.M., Slack P.D., Zorin Y.A., Mor-dvinova V.V., Kozhevnikov V.M., 2003. Evidence for Small-Scale Mantle Convection in the Upper Mantle beneath the Baikal Rift Zone. *Journal of Geophysical Research: Solid Earth* 108 (B4), 2194. <https://doi.org/10.1029/2002JB002039>.

Gileva N.A., Melnikova V.I., Radziminovich N.A., Déver-chère J., 2000. Location of Earthquakes and Average Velocity Parameters of the Crust in Some Areas of the Baikal Region. *Russian Geology and Geophysics* 41 (5), 609–615.

Golenetsky S.I., Perevalova G.I., 1988. On the Use of Computers in Integrated Processing of the Data from Seismic Network in the Baikal Zone. In: *A Study on the Search for Earthquake Precursors in Siberia*. Nauka, Novosibirsk, p. 99–108 (in Russian) [Голенецкий С.И., Перевалова Г.И. Об использовании ЭВМ при сводной обработке наблюдений локальной сети сейсмических станций в Байкальской зоне // Исследования по поискам предвестников землетрясений в Сибири. Новосибирск: Наука, 1988. С. 99–108].

Golubev V.A., 2007. Conductive and Convective Heat Transfer in the Baikal Rift Zone. *GEO, Novosibirsk*, 222 p. (in Russian) [Голубев В.А. Кондуктивный и конвективный вынос тепла в Байкальской рифтовой зоне. Новосибирск: Гео, 2007. 222 с.].

Grudin M.I., Chuvashova I.S. (Eds), 2011. *Baikal. Geology. Human*. ISU Publishing House, Irkutsk, 239 p. (in Russian) [Байкал. Геология. Человек // Ред. М.И. Грудин, И.С. Чувашова. Иркутск: Изд-во ИГУ, 2011. 239 с.].

Gvozdkov A.N., 1998. Geochemistry of the Recent Bottom Sediments of Lake Baikal. PhD Thesis (Candidate of Geology and Mineralogy). Irkutsk, 209 p. (in Russian) [Гвоздков А.Н. Геохимия современных донных осадков озера Байкал: Дис. ... канд. геол.-мин. наук. Иркутск, 1998. 209 с.].

Hutchinson D.R., Golmshtok A.J., Zonenshain L.P., Moore T.C., Schol C.A., Klitgord K.D., 1992. Depositional and Tectonic Framework of the Rift Basins of Lake Baikal from Multi-channel Seismic Data. *Geology* 20 (7), 589–592. [https://doi.org/10.1130/0091-7613\(1992\)020<0589:DATFOT>2.3.CO;2](https://doi.org/10.1130/0091-7613(1992)020<0589:DATFOT>2.3.CO;2).

Khain V.E., Lomize M.G., 2005. *Geotectonics with Fundamentals of Geodynamics*. University Book House, Moscow, 500 p. (in Russian) [Хаин В.Е., Ломизе М.Г. Геотектоника с основами геодинамики. М.: Книжный дом «Университет», 2005. 500 с.].

Khlystov O.M., Khabuev A.V., Minami H., Hachikubo A., Krylov A.A., 2018. Gas Hydrates in Lake Baikal. *Limnology and Freshwater Biology* 2018 (1), 66–70. <https://doi.org/10.31951/2658-3518-2018-A-1-66>.

Khlystov O.M., Kononov E.E., Khabuev A.V., Belousov O.V., Gubin N.A., Solovyeva M.A., Naudts L., 2016. Geological and Geomorphological Characteristics of the Posolsky Bank and the Kukuy Griva, Lake Baikal. *Russian Geology and Geophysics* 57 (12), 1759–1767. <https://doi.org/10.1016/j.rgg.2016.11.001>.

Koulakov I., 2009. LOTOS Code for Local Earthquake Tomographic Inversion: Benchmarks for Testing Tomographic Algorithms. *Bulletin of the Seismological Society of America* 99 (1), 194–214. <https://doi.org/10.1785/0120080013>.

Koulakov I., Tychkov S., Bushenkova N., Vasilevsky A., 2002. Structure and Dynamics of the Upper Mantle beneath the Alpine–Himalayan Orogenic Belt, from Teleseismic Tomography. *Tectonophysics* 358 (1–4), 77–96. [https://doi.org/10.1016/S0040-1951\(02\)00418-3](https://doi.org/10.1016/S0040-1951(02)00418-3).

Krylov S.V., 1980. On Depths of the Baikal Earthquakes and Factors Controlling Seismicity. *Russian Geology and Geophysics* 5, 97–112 (in Russian) [Крылов С.В. О глубинах байкальских землетрясений и сейсмоконтролирующих факторах // Геология и геофизика. 1980. № 5. С. 97–112].

Kulakov I.Yu., 1999. Three-Dimensional Seismic Heterogeneities beneath the Baikal Region According to Data of Local Teleseismic Tomography. *Russian Geology and Geophysics* 40 (3), 317–331 (in Russian) [Кулаков И.Ю. Трехмерные сейсмические неоднородности под Байкальским регионом по данным локальной и телесеismicской томографии // Геология и геофизика. 1999. Т. 40. № 3. С. 317–331].

Kulakov I.Yu., 2008. Upper Mantle Structure beneath Southern Siberia and Mongolia, from Regional Seismic Tomography. *Russian Geology and Geophysics* 49 (3), 187–196. <https://doi.org/10.1016/j.rgg.2007.06.016>.

Lesne O., Calais E., Deverchère J., Chéry J., Hassani R., 2000. Dynamics of Intracontinental Extension in the North Baikal Rift from Two-Dimensional Numerical Deformation Modeling. *Journal of Geophysical Research: Solid Earth* 105 (B9), 21727–21744. <https://doi.org/10.1029/2000JB900139>.

Levi K.G., Babushkin S.M., Badardinov A.A., Buddo V.Y., Larkin G.V., Miroshnichenko A.I., Colman S., 1995. Active Baikal Tectonics. *Russian Geology and Geophysics* 36 (10), 143–154.

Levi K.G., Miroshnichenko A.I., Sankov V.A., Babushkin S.M., Larkin G.V., Badardinov A.A., Wong H.K., Colman S., Delvaux D., 1997. Active Faults of the Baikal Depression. *Bulletin des Centres de Recherches Elf Exploration Production* 21 (2), 399–434.

Logachev N.A., 1974. The Sayan-Baikal and Stanovoe Highlands. In: N.A. Florensov (Ed.), *Highlands of Pribaikalia and Transbaikalia*. Nauka, Moscow, p. 16–162 (in Russian) [Логачев Н.А. Саяно-Байкальское становое нагорье // Нагорья Прибайкалья и Забайкалья / Ред. Н.А. Флоренсов. М.: Наука, 1974. С. 16–162].

Logatchev N.A., 1993. History and Geodynamics of the Lake Baikal Rift in the Context of the Eastern Siberia Rift System: A Review. *Bulletin des Centres de Recherches Elf Exploration Production* 17 (2), 353–370.

Logachev N.A., 1999. Main Structural Features and Geodynamics of the Baikal Rift Zone. *Physical Mesomechanics* 2 (1–2), 163–170 (in Russian) [Логачев Н.А. Главные структурные черты и геодинамика Байкальской рифтовой зоны // Физическая мезомеханика. 1999. Т. 2. № 1–2. С. 163–170].

Logachev N.A., 2001. On Historical Core of the Baikal Rift Zone. *Doklady Earth Sciences* 376 (4), 510–513 (in Russian) [Логачев Н.А. Об историческом ядре Байкальской рифтовой зоны // Доклады АН. 2001. Т. 376. № 4. С. 510–513].

Logachev N.A., 2003. History and Geodynamic of the Baikal Rift. *Russian Geology and Geophysics* 44 (5), 391–406.

Logatchev N.A., Zorin Yu.A., 1987. Evidence and Causes of the Two-Stage Development of the Baikal Rift. *Tectonophysics* 143 (1–3), 225–234. [https://doi.org/10.1016/0040-1951\(87\)90092-8](https://doi.org/10.1016/0040-1951(87)90092-8).

Lukhnev A.V., Sankov V.A., Miroshnichenko A.I., Ashurkov S.V., Byzov L.M., Sankov A.V., Bashkuev Yu.B., Dembelov M.G., Calais E., 2013. GPS-Measurements of Recent Crustal Deformation in the Junction Zone of the Rift Segments in the Central Baikal Rift System. *Russian Geology and Geophysics* 54 (11), 1417–1426. <https://doi.org/10.1016/j.rgg.2013.10.010>.

Lunina O.V., 2016. The Digital Map of the Pliocene–Quaternary Crustal Faults in the Southern East Siberia and the Adjacent Northern Mongolia. *Geodynamics & Tectonophysics* 7 (3), 407–434 (in Russian) [Лунина О.В. Цифровая карта разломов для плиоцен-четвертичного этапа развития земной коры юга Восточной Сибири и сопредельной территории Северной Монголии // Геодинамика и тектонофизика. 2016. Т. 7. № 3. С. 407–434]. <https://doi.org/10.5800/GT-2016-7-3-0215>.

Lunina O.V., Andreev A.V., Gladkov A.S., 2012. The Tsagan Earthquake of 1862 on Lake Baikal Revisited: A Study of Secondary Coseismic Soft-Sediment Deformation. *Russian Geology and Geophysics* 53 (6), 594–610. <https://doi.org/10.1016/j.rgg.2012.04.007>.

Lunina O.V., Gladkov A.S., Nevedrova N.N., 2009. Rift Basins in Pribaikalie: Tectonic Structure and Development History. *GEO, Novosibirsk*, 316 p. (in Russian) [Лунина О.В., Гладков А.С., Неведрова Н.Н. Рифтовые впадины Прибайкалья: тектоническое строение и история развития. Новосибирск: Гео, 2009. 316 с.].

Lunina O.V., Gladkov A.S., Sherstyankin P.P., 2010. A New Electronic Map of Active Faults for Southeastern Siberia. *Doklady Earth Sciences* 433, 1016–1021. <https://doi.org/10.1134/S1028334X10080064>.

Mats V.D., 2012. The Sedimentary Fill of the Baikal Basin: Implications for Rifting Age and Geodynamics. *Russian Geology and Geophysics* 53 (9), 936–954. <https://doi.org/10.1016/j.rgg.2012.07.009>.

Mats V.D., 2015. The Baikal Rift: Pliocene (Miocene) – Quarternary Episode or Product of Extended Development since the Late Cretaceous under Various Tectonic Factors. A

Review. *Geodynamics & Tectonophysics* 6 (4), 467–490 (in Russian) [Мац В.Д. Байкальский рифт: плиоцен (миоцен) – четвертичный эпизод или продукт длительного развития с позднего мела под воздействием различных тектонических факторов. Обзор представлений // Геодинамика и тектонофизика. 2015. Т. 6. № 4. С. 467–490]. <https://doi.org/10.5800/GT-2015-6-4-0190>.

Mats V.D., Ufimtsev G.F., Mandelbaum M.M., Alakshin A.M., Pospeev A.V., Shimaraev M.N., Khlystov O.M., 2001. The Cenozoic Baikal Rift Basin: Its Structure and Geological History. *GEO, Novosibirsk*, 252 p. (in Russian) [Мац В.Д., Уфимцев Г.Ф., Мандельбаум М.М., Алакшин А.М., Поспеев А.В., Шимараев М.Н., Хлыстов О.М. Кайнозой Байкальской рифтовой впадины: строение и геологическая история. Новосибирск: Гео, 2001. 252 с.].

Melnikova V.I., Radziminovich N.A., 1998. Focal Mechanisms of the Earthquakes of the Baikal Region for 1991–1996. *Russian Geology and Geophysics* 39 (11), 1598–1607 (in Russian) [Мельникова В.И., Радзиминович Н.А. Механизм очагов землетрясений Байкальского региона за 1991–1996 гг. // Геология и геофизика. 1998. Т. 39. № 11. С. 1598–1607].

Misharina L.A., Melnikova V.I., Baljinnyam I., 1983. Southwestern Boundary of the Baikal Rift Zone from the Data on Earthquake Focal Mechanisms. *Volcanology and Seismology* 2, 74–83 (in Russian) [Мишарина Л.А., Мельникова В.И., Балжинням И. Юго-западная граница Байкальской рифтовой зоны по данным о механизме очагов землетрясений // Вулканология и сейсмология. 1983. № 2. С. 74–83].

Misharina L.A., Solonenko N.V., 1972. On Stresses at Small Earthquake Sources in Pribaikalye. *Bulletin of the USSR Academy of Sciences. Physics of the Earth* 4, 24–36 (in Russian) [Мишарина Л.А., Солоненко Н.В. О напряжениях в очагах слабых землетрясений Прибайкалья // Известия АН СССР. Физика Земли. 1972. № 4. С. 24–36].

Misharina L.A., Solonenko N.V., 1977. Earthquake Focal Mechanisms and Stressed State of the Earth's Crust in the Baikal Rift Zone. In: N.A. Logachev, N.A. Florensov (Eds), *A Role of Rifting in Geological History of the Earth*. Nauka, Novosibirsk, p. 120–125 (in Russian) [Мишарина Л.А., Солоненко Н.В. Механизм очагов землетрясений и напряженное состояние земной коры в Байкальской рифтовой зоне // Роль рифтогенеза в геологической истории Земли / Ред. Н.А. Логачев, Н.А. Флоренсов. Новосибирск: Наука, 1977. С. 120–125].

Mordvinova V.V., Vinnik L.P., Kosarev G.L., Oreshin S.I., Treusov A.V., 2000. Teleseismic Tomography of the Baikal Rift Lithosphere. *Doklady Earth Sciences* 372 (4), 716–720.

Nevedrova N.N., Epov M.I., 2004. Analysis of Electromagnetic Monitoring Results at Baikal Prognostic Test-Site. *NNC RK Bulletin* 2, 143–149 (in Russian) [Неведрова Н.Н., Эпов М.И. Анализ результатов электромагнитного мониторинга на Байкальском прогностическом полигоне // Вестник НЯЦ РК. 2004. № 2. С. 143–149].

Nicolas A., Achauer U., Daignieres M., 1994. Rift Initiation by Lithospheric Rupture. *Earth and Planetary Science*

Letters 123 (1–3), 281–298. [https://doi.org/10.1016/0012-821X\(94\)90274-7](https://doi.org/10.1016/0012-821X(94)90274-7).

Nolet G. (Ed.), 1990. Seismic Tomography. With Applications in Global Seismology and Explorational Geophysics. Mir, Moscow, 416 p. (in Russian) [Сейсмическая томография: с приложениями в глобальной сейсмологии и разведочной геофизике / Ред. Г. Нолет. М.: Мир, 1990. 416 с.].

Peltzer G., Tapponnier P., 1988. Formation and Evolution of Strike-Slip Faults, Rifts, and Basins during the India-Asia Collision: An Experimental Approach. *Journal of Geophysical Research: Solid Earth* 93 (B12), 15085–15117. <https://doi.org/10.1029/JB093iB12p15085>.

Petit C., Koulakov I., Deverchère J., 1998. Velocity Structure around the Baikal Rift Zone from Teleseismic and Local Earthquake Traveltimes and Geodynamic Implications. *Tectonophysics* 296 (1–2), 125–144. [https://doi.org/10.1016/S0040-1951\(98\)00140-1](https://doi.org/10.1016/S0040-1951(98)00140-1).

Radziminovich N.A., 2010. Focal Depths of Earthquakes in the Baikal Region: A Review. *Izvestiya, Physics of the Solid Earth* 46, 216–229. <https://doi.org/10.1134/S1069351310030043>.

Sankov V.A., Lukhnev A.V., Miroshnichenko A.I., Levi K.G., Ashurkov S.V., Bashkuev Yu.B., Dembelov M.G., Calais E., Déverchère J., Vergnolle M., Bechtur B., Amarjargal Ch., 2003. Present-Day Movements of the Earth's Crust in the Mongol-Siberian Region Inferred from GPS Geodetic Data. *Reports of the Academy of Sciences* 393 (8), 1082–1085.

Scholz C.A., Hutchinson D.R., 2000. Stratigraphic and Structural Evolution of the Selenga Delta Accommodation Zone, Lake Baikal Rift, Siberia. *International Journal of Earth Sciences* 89, 212–228. <https://doi.org/10.1007/s00531000095>.

Shchetnikov A.A., Radziminovich Y.B., Vologina E.G., Ufimtsev G.F., 2012. The Formation of Proval Bay as an Episode in the Development of the Baikal Rift Basin: A Case Study. *Geomorphology* 177–178, 1–16. <http://doi.org/10.1016/j.geomorph.2012.07.023>.

Sherman S.I., Levi K.G., 1977. Transform Faults of the Baikal Rift Zone. *Doklady of the USSR Academy of Sciences* 233 (2), 461–464 (in Russian) [Шерман С.И., Леви К.Г. Трансформные разломы Байкальской рифтовой зоны // Доклады АН СССР. 1977. Т. 233. № 2. С. 461–464].

Sherman S.I., Lysak S.V., Gorbunova E.A., 2012. A Tectonophysical Model of the Baikal Seismic Zone: Testing and Implications for Medium-Term Earthquake Prediction. *Russian Geology and Geophysics* 53 (4), 392–405. <https://doi.org/10.1016/j.rgg.2012.03.003>.

Solonenko V.P. (Ed.), 1981. Seismogeology and Detailed Seismic Zoning of Pribaikalye. Nauka, Novosibirsk, 168 p. (in Russian) [Сейсмогеология и детальное сейсмическое районирование Прибайкалья / Ред. В.П. Солоненко. Новосибирск: Наука, 1981. 168 с.].

Song Y., Krylov S.V., Yang B., Cai L., Dong S., Liang T., Li J., Xu X., Mishenkina Z.R., Petrik G.V., Shelud'ko I.F., Seleznev V.S.,

Solov'ev V.M., 1996. Deep Seismic Sounding of the Lithosphere on the Baikal – Northeastern China International Transect. *Russian Geology and Geophysics* 37 (2), 3–15 (in Russian) [Сун Юншен, Крылов С.В., Ян Баоцзюнь, Лю Цай, Дун Шисюэ, Лян Течен, Ли Цзинчжи, Сюй Синчжуи, Мишенькина З.Р., Петрик Г.В., Шелудько И.Ф., Се-лезнев В.С., Соловьев В.М. Глубинное сейсмическое зон-дирование литосферы на международном трансекте Байкал – Северо-Восточный Китай // Геология и гео-физика. 1996. Т. 37. № 2. С. 3–15].

State Geological Map of the Russian Federation, 2009. Angara-Yenisei Series. Scale 1:1000000. Sheet N-48 (Irkutsk). Explanatory Note. VSEGEI Publishing House, Saint Petersburg, 574 p. (in Russian) [Государственная геологи-ческая карта Российской Федерации. Серия Ангаро-Енисейская. Масштаб 1:1000000. Лист N-48 (Иркутск): Объяснительная записка. СПб.: Изд-во ВСЕГЕИ, 2009. 574 с.].

Suvorov V.D., Mishen'kina Z.R., 2005. Structure of Sedi-mentary Cover and Basement beneath the South Basin of Lake Baikal Inferred from Seismic Profiling. *Russian Geology and Geophysics* 46 (11), 1141–1149.

Suvorov V.D., Tubanov T.A., 2008. Distribution of Local Earthquakes in the Crust beneath Central Lake Baikal. *Russian Geology and Geophysics* 49 (8), 611–620. <http://doi.org/10.1016/j.rgg.2007.09.019>.

Ten Brink U.S., Taylor M.H., 2002. Crustal Structure of Central Lake Baikal: Insights into Intracontinental Rifting. *Journal of Geophysical Research: Solid Earth* 107 (B7), 2132. <https://doi.org/10.1029/2001JB000300>.

Tiberi C., Diamant M., Déverchère J., Petit-Mariani C., Mikhailov V., Tikhotsky S., Achauer U., 2003. Deep Structure of the Baikal Rift Zone Revealed by Joint Inversion of Gravity and Seismology. *Journal of Geophysical Research: Solid Earth* 108 (B3), 2133. <http://doi.org/10.1029/2002jb001880>.

Yakovlev A.V., Koulakov I.Yu., Tychkov S.A., 2007. Moho Depths and Three-Dimensional Velocity Structure of the Crust and Upper Mantle beneath the Baikal Region, from Local Tomography. *Russian Geology and Geophysics* 48 (2), 204–220. <http://doi.org/10.1016/j.rgg.2007.02.005>.

Zhao D., Lei J., Inoue T., Yamada A., Gao S.S., 2006. Deep Structure and Origin of the Baikal Rift Zone. *Earth and Plane-tary Science Letters* 243 (3–4), 681–691. <https://doi.org/10.1016/j.epsl.2006.01.033>.

Zonenshain L.P., Savostin L.A., 1981. Geodynamics of the Baikal Rift Zone and Plate Tectonics of Asia. *Tectono-physics* 76 (1–2), 1–45. [https://doi.org/10.1016/0040-1951\(81\)90251-1](https://doi.org/10.1016/0040-1951(81)90251-1).

Zorin Yu.A., Turutanov E.Kh., 2005. Plumes and Geody-namics of the Baikal Rift Zone. *Russian Geology and Geo-physics* 46 (7), 685–699 (in Russian) [Зорин Ю.А., Туру-танов Е.Х. Плумы и геодинамика Байкальской риф-товой зоны // Геология и геофизика. 2005. Т. 46. № 7. С. 685–699].

APPENDIX 1

SYNTHETIC TESTS

Repeated testing was performed to validate the inversion results for the experimental data.

The resolution was validated through synthetic testing with chess-board anomalies. The procedure of this test is as follows. There has been created a synthetic velocity model which consists of alternating positive and negative anomalies of the prescribed size and looks like a chess board. The direct model-related problem to be solved is to calculate travel times for distribution of seismicity and location of stations from the catalog studied. After that, an inverse problem in tomography is to be solved based on the travel times obtained.

There have been conducted checkerboard tests with different sizes of anomalies in the amplitude of $\pm 5\%$ for checking the horizontal resolution. Fig. 1 shows the results for anomalies with dimensions of 30×30 km. It can be seen that amplitude and shape of the anomalies with such dimensions are reconstructable to a depth of 20 km wherever the inversion is performed. A similar test for anomalies with less dimensions (25×25 km) showed that they become vague with depth. Thus, the testing results

allowed concluding that the anomalies with horizontal dimensions of 30 km and greater can be determined reliably to a depth of 20 km. The vertical resolution was checked by assigning the model along the vertical segments with alternating anomalies in the amplitude of $\pm 10\%$, with a width of 30 km and change of sign at a depth of 15 km. The anomalies of such dimensions and a contrast transition based on sign change at depth were also reconstructed.

Synthetic tests make it possible to choose optimal parameters for inversion performance. A sustainable solution (the absence of any other anomalies) can be based on the following parameter values: horizontal and vertical smoothing (1.0 for P-waves and 2.0 for S-waves), and amplitude damping (0.6 for P-waves and 1.0 for S-waves).

To estimate the reliability of identifying anomalies and the impact of random noise on the tomography results, there was a test on even and odd source numbers, with the inversion performed separately for these two independent samples from the initial catalog. The test results show a good correlation between the anomalies identified.

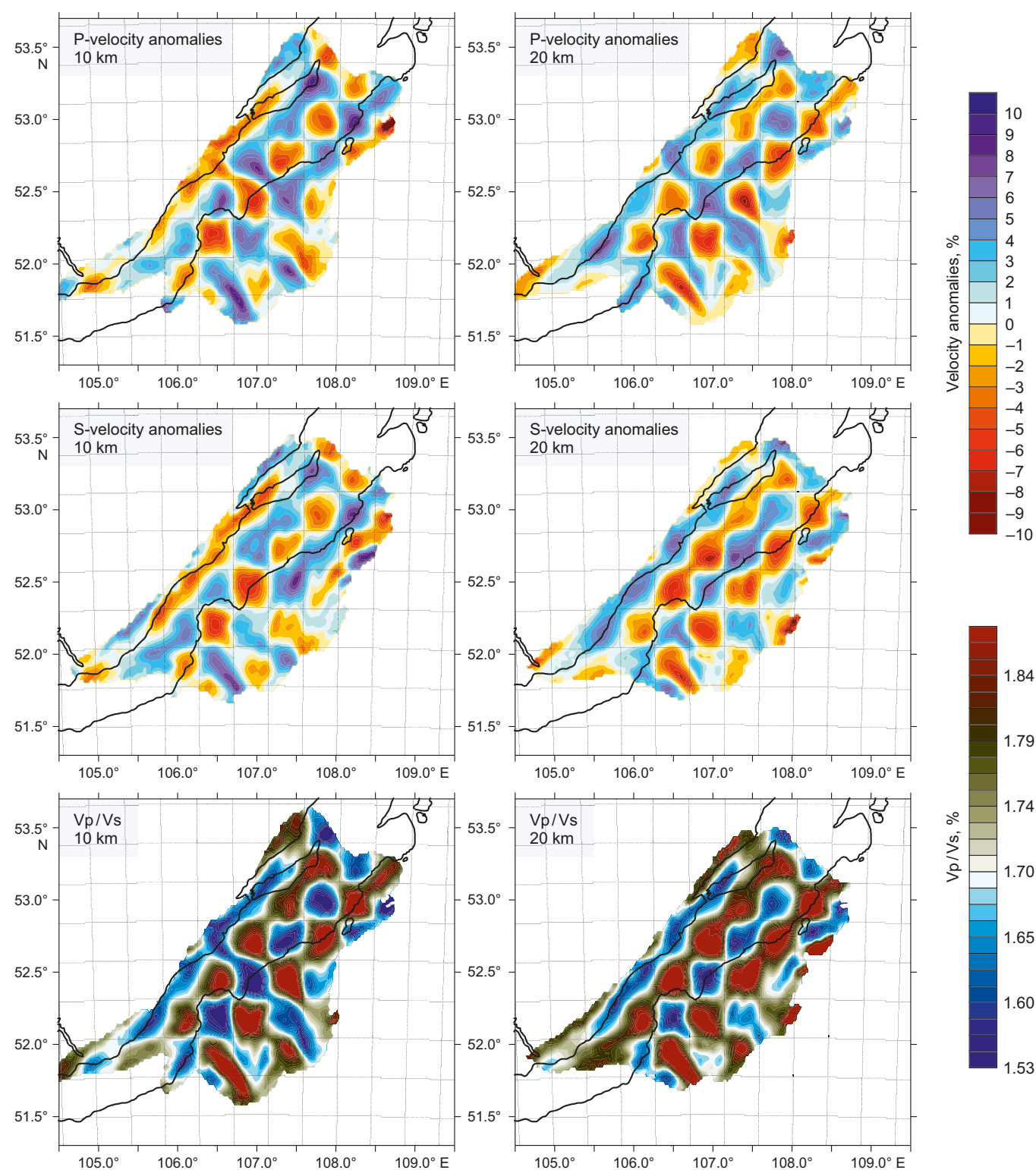


Fig. 1.1. The result of reconstructing synthetic anomalies of size 30×30 km for the study area at depths of 10 and 20 km.